Experimental Evaluation of Ground-Based Microwave Radiometric Sensing of Atmospheric Temperature and Water Vapor Profiles

M. T. DECKER, E. R. WESTWATER AND F. O. GUIRAUD

NOAA/ERL/Wave Propagation Laboratory, Boulder, CO 80302

(Manuscript received 13 January 1978, in final form 16 September 1978)

ABSTRACT

Profiles of atmospheric temperature and water vapor derived from ground-based microwave radiometric measurements are compared with concurrent rawinsonde profiles including both clear and cloudy cases. Accuracies of the temperature profiles including the cloudy cases are quite close to predicted accuracies. Mean virtual temperatures between commonly used pressure levels are also compared and resulting rms accuracies are 1.1, 1.6, 2.0 and 2.8°C for the 1000–850, 850–700, 700–500 and 500–300 mb layers, respectively. The microwave technique is potentially useful in applications requiring high time resolution or in data-sparse regions of the oceans that might be covered by an ocean data buoy system.

1. Introduction

Thermal radiation from the atmosphere at microwave frequencies originates primarily from oxygen, water vapor and liquid water, and depends on their temperature and spatial distribution. For a well-mixed gas such as oxygen, and given the surface pressure, the radiation contains information primarily on the atmospheric temperature. It is thus possible to infer temperature structure from surface-based radiation measurements in the 60 GHz oxygen absorption complex. These measurements are "contaminated" by radiation from water vapor and especially from cloud liquid. Hence improved accuracy and operation during cloudy conditions are possible if measurements are also made of radiation from these constituents at frequencies outside the oxygen band. In addition to their use in temperature profiling these observations can be used to infer line integrals of water vapor and cloud liquid. In some cases vapor profile information can also be obtained.

Previous field experiments (Hosler and Lemmons, 1972; Miner *et al.*, 1972; Snider, 1972; Westwater *et al.*, 1975; Gurvich and Yershov, 1976) demonstrated that, under clear conditions, smoothed features of vertical temperature profiles can be recovered. Westwater *et al.* (1976) used a computer simulation to examine the feasibility of sensing temperature profiles from ocean data buoys. This study presented methods for correcting measurements for the radiation from clouds and water vapor, and concluded that useful data could be obtained under both clear and cloudy conditions. As a further step in this evaluation a series of field experiments has been carried out jointly by NOAA and the Jet Propulsion Laboratory. The purpose of these experiments was to confirm our ability to predict accuracies of radiometrically derived temperature profiles for a known season and geographical locations, especially under cloudy conditions. We present here a comparison of 88 simultaneous rawinsonde and radiometer temperature and water vapor profiles. Clouds were present in 54 of these cases and the cloud-correction techniques are shown to reduce the temperature profile errors very nearly to those expected in the clear-sky cases.

2. Experiment description

Measurements were made at the Pacific Missile Test Center (PMTC), Pt. Mugu, California, during the periods 24 February–17 March and 16–30 July 1976. The 21 profiles analyzed for the first period were all under essentially clear skies; 16 of 22 profiles during the second period were classified as cloudy. A more severe environmental test was made aboard the Canadian Ship *Quadra* at Ocean Station P in the Gulf of Alaska from 15 February–26 March 1977. Of the 45 profiles from this location 35 were cloudy.

The microwave radiometer, operated by personnel from the Jet Propulsion Laboratory, is similar to that used on the Nimbus 6 satellite (Staelin *et al.*, 1975). It has three channels in the oxygen absorption band at 52.85, 53.85 and 55.45 GHz, one channel in the water vapor absorption line at 22.235 GHz, and a window channel at 31.65 GHz. The radiometer was operated in an angular scan mode over ±45° from the zenith in steps of 7.5°. Dwell time at each zenith angle is 1 s with the sequence being repeated approximately once each minute. The antennas also scan temperature-controlled targets which are used together

with the angular-scan data for calibration purposes. Although radiation from the various zenith angles could be used in retrieving atmospheric profiles, we have restricted ourselves to zenith-pointing data because of the difficulty in correcting for buoy motion in an operational system. In general, 18 to 24 of the measurements at 1 min intervals were averaged to give the radiation data used in retrieval of profiles. In addition to the five channels of radiometric data, surface measurements of temperature, pressure and relative humidity available from regular rawinsonde launch procedures were used in our profile retrievals.

Rawinsondes used for comparison purposes were routine launches by personnel of the PMTC for the Pt. Mugu measurements and by personnel of the *Quadra* for the Gulf of Alaska measurements. The radiometers were at the rawinsonde release location in all cases. Radiometric measurements began at rawinsonde release time in all but three cases; in these three instances (aboard the *Quadra*) time differences were less than 1 h.

3. Analysis

Statistical retrieval algorithms have been used extensively to extract temperature profiles from both microwave (Waters *et al.*, 1975; Westwater *et al.*, 1975; Yershov *et al.*, 1975) and infrared (Smith *et al.*, 1970; Rodgers, 1970) radiation measurements. These algorithms also predict retrieval accuracies if realistic estimates of measurement uncertainties are known.

Previous experiments have used thermal emission in the oxygen complex under clear-sky conditions to determine temperature profiles. Cloud emission, however, can introduce non-negligible departures from the corresponding emission from clear air for the upward-looking case. Microwave emission below about 45 GHz is insensitive to temperature structure and depends strongly on water, so measurements at the lower frequencies may be used to correct for the effects of clouds. Since the lower frequency emission depends on both water vapor and liquid water, two frequencies are required. As described by Westwater *et al.* (1976), our technique is to estimate the equivalent clear air radiation from the cloudy measurements both within and outside the oxygen band. Similar work has been published by Fowler *et al.* (1975). In a procedure identical to our commonly used profile retrieval algorithm, we use an eight-element data vector consisting of the five cloudy radiation measurements and surface temperature, pressure and relative humidity (and perhaps higher order products of these quantities) as a minimum variance estimator of the equivalent clear air radiation for the five radiometer channels. In this algorithm the statistical ensemble is representative of cloudy atmospheres only. The resulting data sets representing equivalent radiation from a clear sky may then be used in an inversion algorithm constructed from a statistical ensemble of clear profiles to retrieve temperature and water vapor profiles. The equivalent clear sky radiation may be used with an effective noise level different from that used with measurements under clear sky conditions, depending on frequency and the range of liquid water thickness present in the cloud ensemble. In using the above algorithm we assume that it is known whether or not clouds are present. This initial categorization is made by using the same eight-element data vector as above to determine the integrated amounts of liquid water and water vapor. The measurement is classified as cloudy if the inferred liquid amount exceeds some threshold, usually taken to be an integrated thickness of 20 μm. The statistical ensemble upon which this algorithm is based includes a representative sample of both clear and cloudy profiles.

In summary, our analysis uses statistical retrieval algorithms 1) to determine the integrated amount of cloud liquid and water vapor, and thus categorize the sky at the time of measurement as clear or cloudy; 2) to estimate, for cloudy cases, the equivalent radiation from the clear atmosphere; and 3) to retrieve temperature and water vapor profiles.

To eliminate biases that might arise from the instruments or from incorrect absorption coefficients, we forced averages of measured and calculated brightness temperatures for a sample of clear sky cases to agree. The brightness temperature calculations were made using contemporary absorption models and assuming the rawinsonde profiles were correct. Since different instruments were used in the three experimental runs, the corrections were made separately for each run. From 11 clear cases in the first run, 5 in the second and 10 in the third, the bias adjustments listed in Table 1 were calculated and applied to radiometric data of each run. These cases are included in the statistical summaries presented later. The standard deviations after the biases have been subtracted are also included in Table 1.

TABLE 1. Brightness temperature bias adjustments.

Frequency (GHz)	22.235	31.65	52.85	53.85	55.45
Pt. Mugu, Feb–Mar 1976 ($n=11$)					
Bias (K)	−2.8	−1.7	−0.2	−0.1	+1.2
Standard deviation (K)	2.2	0.7	1.5	0.7	0.5
Pt. Mugu, July 1976 ($n=5$)					
Bias (K)	−4.0	+0.1	−2.3	−3.8	+1.2
Standard deviation (K)	1.7	1.1	0.8	1.6	0.4
Gulf of Alaska, Feb–Mar 1977 ($n=10$)					
Bias (K)	−1.6	−1.0	+1.1	−0.1	−1.0
Standard deviation (K)	2.5	1.6	1.1	0.6	0.4

4. Cloud models

Construction of algorithms of the previous section require representative ensembles of cloud conditions, in-

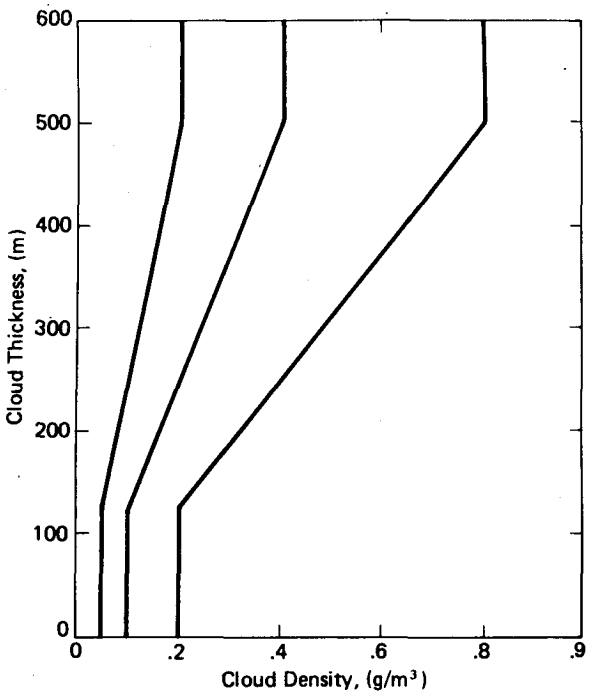

FIG. 1. Cloud thickness-liquid density models used in thermal emission simulations.

cluding realistic statistical distributions of base height, thickness, liquid water content, temperature, etc. Our ensembles were obtained by inserting clouds into our *a priori* set of rawinsonde data if at any point the relative humidity exceeded 95%. Base heights were taken to be the (interpolated) levels at which the humidity first exceeded 95% and thicknesses were determined using the points at which the humidity dropped below 95%. Some profiles will contain two or more cloud layers. Since liquid density is not measured by rawinsondes, completion of our ensemble required modeling of this parameter. We assumed that the liquid density within a given cloud was constant with height. For each cloudy rawinsonde profile we picked three values of density, one from each of the cloud thickness-liquid density models of Fig. 1. These models cover a reasonable range of observed liquid densities for non-precipitating clouds, and restrict thin clouds to low densities. Each rawinsonde profile with relative humidity above 95% was therefore used to generate four profiles—a clear case, and three cases with different liquid densities. Westwater *et al.* (1976) show the resulting distributions of cloud parameters for five ocean weather stations. The wide range of variation of these parameters provides a stringent test of our hypothesis that we can correct for clouds without knowledge of the details of cloud structure. The study shows that the accuracy to which clear air emission can be inferred from a set of cloud-contaminated emission measurements closely approaches the instrumental noise level for frequencies above 54 GHz. Below this frequency the effective noise level increases and should be considered in assigning errors to the statistical ensemble used for generating the profile retrieval algorithms.

Statistical ensembles of atmospheric profiles for the PMTC February–March experiment reported in this paper are derived from archived Pt. Mugu rawinsondes for the two 3-month periods February–March–April of 1973 and 1974. June–July–August data for the same years are used for the second experimental period. February–March–April data of 1966 and 1967 from Ocean Station P are used for the third period.

5. Results

Examples of retrieved temperature and water vapor profiles are shown in Fig. 2. Height on the vertical scale is given in pressure difference from the surface. Note that a pressure difference of 100 mb corresponds to a geometrical height of about 0.9 km, 300 mb to 3 km, 500 mb to 5.6 km and 800 mb to 12 km. Point values are retrieved at 10 mb increments in these profiles.

These examples indicate the characteristic smoothing of the radiometric profiles, especially for elevated temperature structure and for water vapor at all heights. We note that this system is not designed specifically for water vapor profile retrieval. Radiometric data for the examples on 16 and 22 July indicated that clouds were present with equivalent liquid thickness of 150 and 327 μm, respectively. Clouds with this liquid amount contribute significantly to radiation in the radiometric channels other than that at 55.45 GHz.

Fig. 3 shows the theoretical accuracies (curves with prefix T) in profile retrieval expected for the appropriate clear sky climatology and an rms instrument accuracy of 1 K together with the achieved accuracies during the three experimental periods (curves with prefix E). The rms error in retrieved profiles is taken to be the rms difference between the rawinsonde values and the radiometrically retrieved values. Thus, we assume that there are no errors in the rawinsonde measurements. Curves labeled T3 are the theoretical accuracies expected if the mean of the *a priori* statistical ensemble is used as the predictor of all profiles, i.e., no measurement is made. This then is the standard deviation of the *a priori* ensemble about its mean. Curves E3 are the corresponding experimentally observed quantities, i.e., the rms difference between the *a priori* mean and the rawinsonde profiles for the experimental cases. If surface values of temperature, pressure and relative humidity are used as predictors some improvement in accuracy over the *a priori* mean may be obtained as indicated by the curves labeled T2 and E2. Finally, accuracies predicted and actually observed when the full data set of five radiometric channels and three surface quantities are used are given by the curves labeled T1 and E1.

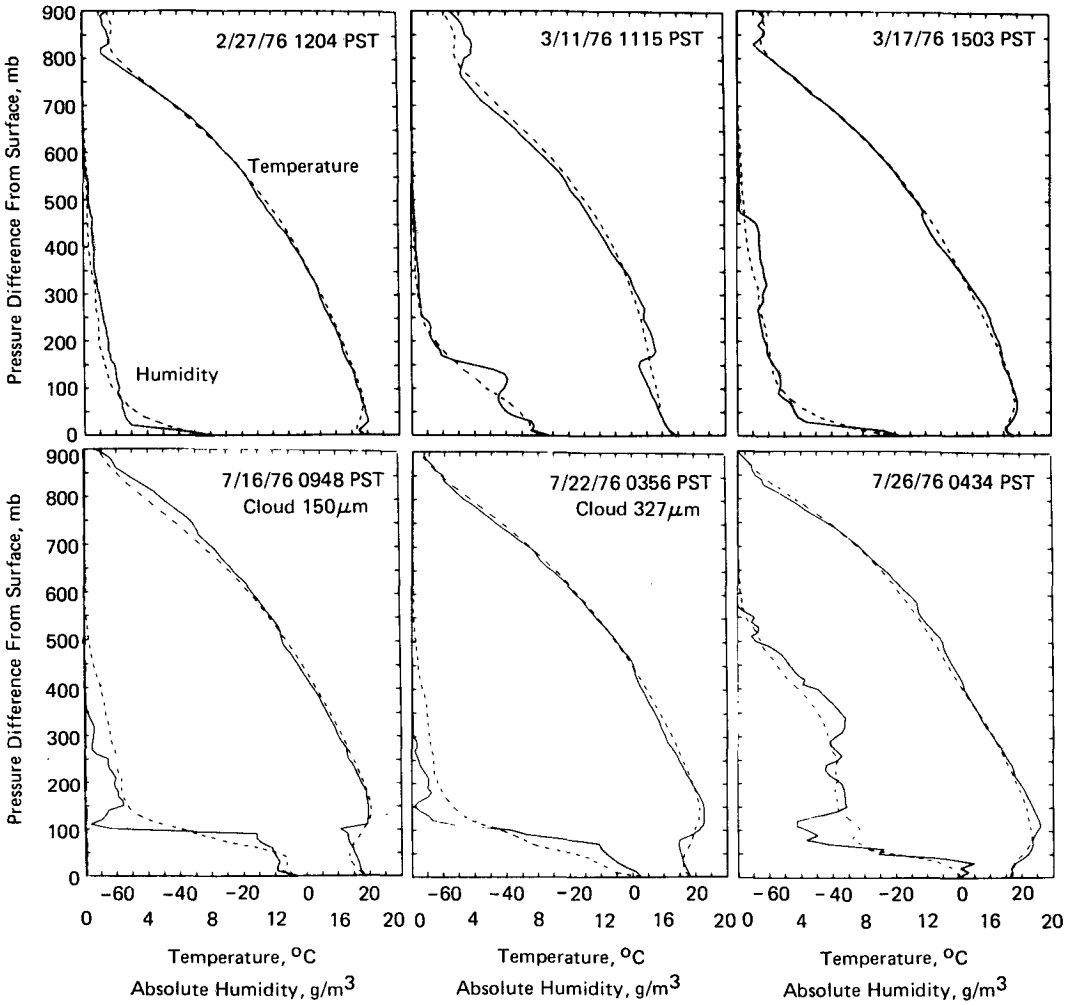

FIG. 2. Examples of retrievals of temperature and water vapor profiles. Solid lines, rawinsonde; dashed lines, radiometer.

This analysis shows that the achieved temperature profile accuracies are quite close to the theoretical prediction of accuracy. Temperature variations during the February–March experimental period at Pt. Mugu were larger than in the *a priori* sample as indicated by curve E3 of Fig. 3a, but this variance was reduced to the predicted value as shown by curve E1. On the other hand, temperature variations during the PMTC July period were quite small, and except for heights near 100 mb above the surface there is little improvement over the *a priori* mean. This experimental period did have clouds during many of the measurements and provided a test of our cloud-correction algorithm. These clouds were generally low-level stratus with integrated liquids inferred from the radiometric measurements ranging from about 100 to 300 μm; Fig. 4 illustrates the improvement in retrieval accuracies, the curves being similar to the E1 curves of Fig. 3b. It is evident that without the correction for clouds there would be a substantial increase in error and that the correction algorithm effectively eliminates this error.

The third experimental period in the Gulf of Alaska also included a large fraction of cloudy cases with line integrals of liquid up to about 900 μm. The accuracies achieved during the experimental period shown in Fig. 3c agree with the predicted values up to 500 mb pressure difference from the surface, but are somewhat larger at heights just above this as shown by curve E1.

In each of the three experimental periods the temperature error curves imply that significant information is obtained at altitudes well above the 500 mb pressure difference, including altitudes above the tropopause. However, it is likely that this is a result of the correlation of these temperatures with those at lower levels and hence the temperature information at the higher levels would not be reliable in statistically anomalous situations. This is also evident from the shape of the temperature weighting functions for these frequencies which are maximum at the

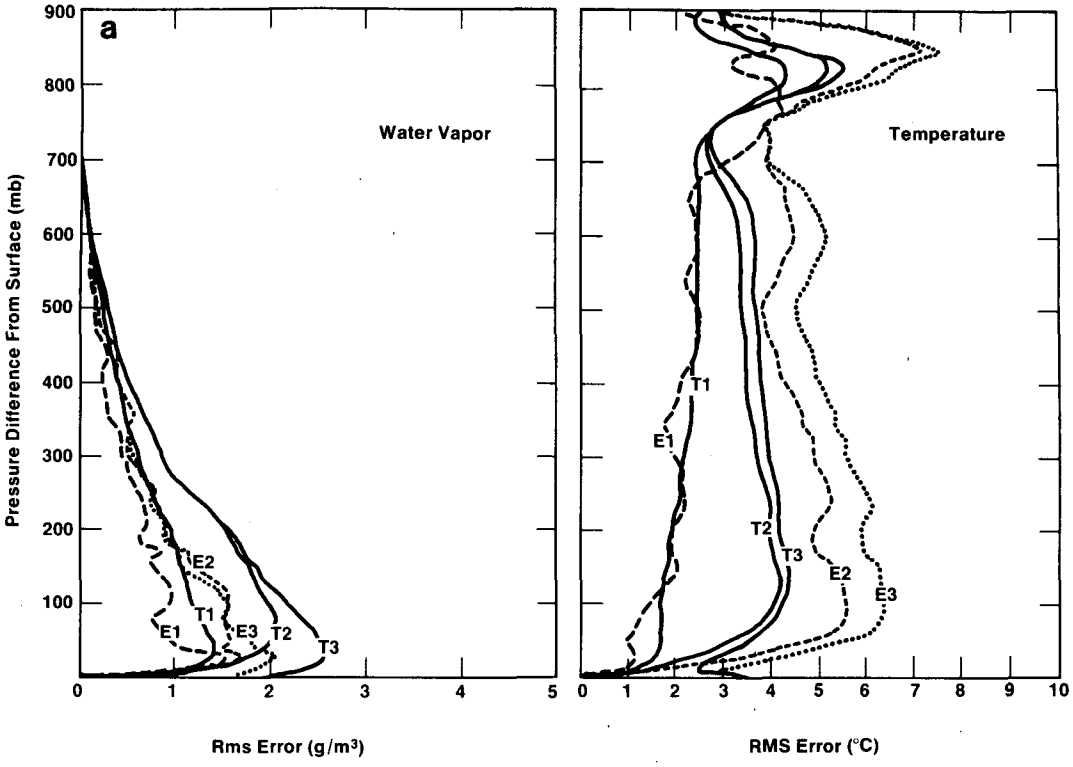

FIG. 3a. Comparison of theoretically predicted and experimentally observed accuracies of temperature and water vapor profiles for Pt. Mugu, February–March 1976. T, theoretical; E, experimental; 1, profiles retrieved using five radiometric channels and surface temperature, pressure and humidity; 2, profiles from surface data only; 3, *a priori* mean.

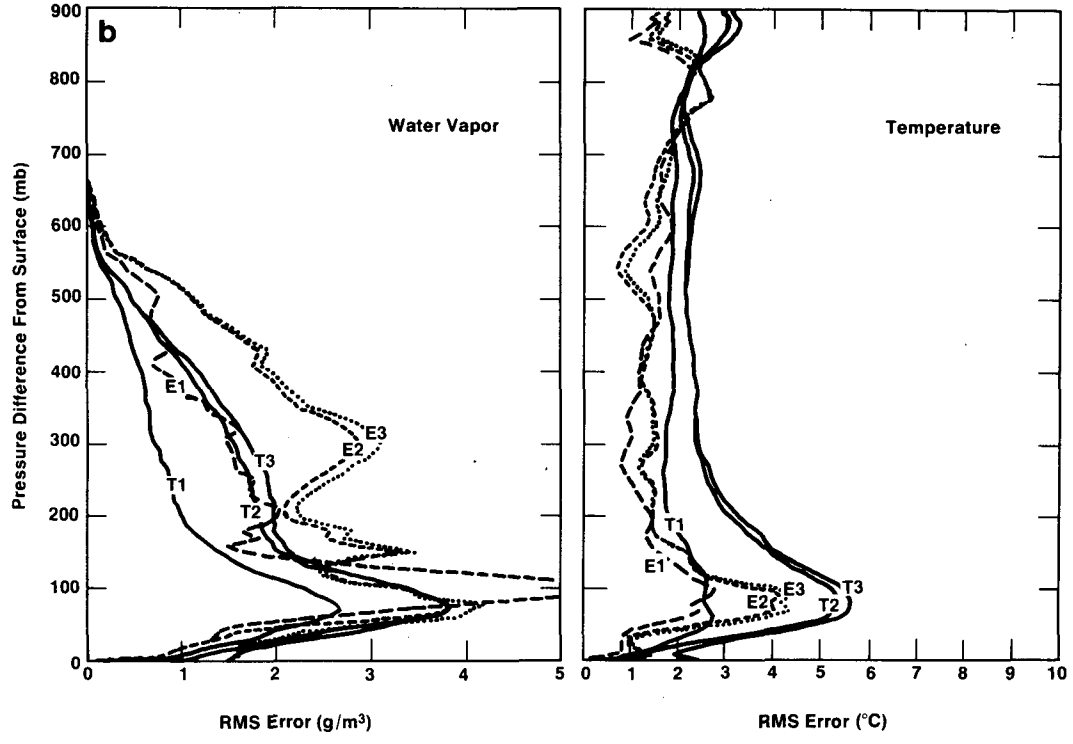

FIG. 3b. As in Figure 3a, except for Pt. Mugu, July 1976.

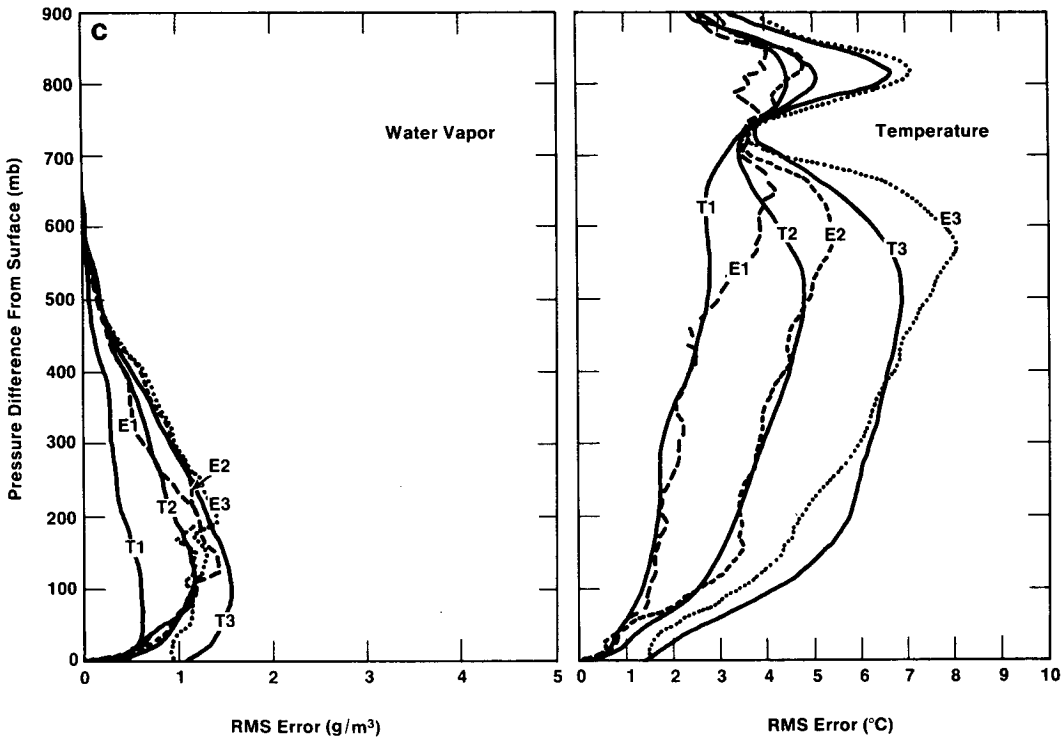

FIG. 3c. As in Figure 3a, except for Gulf of Alaska, February–March 1977.

surface and decrease to very low values at these heights.

The rather large error in temperature and especially water vapor profiles near 100 mb above the surface in the July measurements at Pt. Mugu shown in Fig. 3b is largely the result of the smoothing of the sharp boundary of the marine subsidence inversion. This is illustrated by the July examples of Fig. 2. However, for some meteorological applications, and in particular the numerical models that might use ocean buoy data, average temperatures between specified pressure levels may be used, making the detailed structure less important. We have used the radiometric and rawinsonde profiles to compute the thickness (equivalent to mean virtual temperature) between commonly used pressure levels. These are illustrated in the scatter diagrams of Fig. 5, where data for the three experimental periods are combined. The rms differences between radiometric and rawinsonde thicknesses are given for each layer. The 5.0 m rms difference for the 1000–850 mb layer corresponds to an rms mean temperature difference of 1.1°C. Similarly the 850–700 mb layer corresponds to 1.6°C, the 700–500 mb layer to 2.0°C, and the 500–300 mb layer to 2.8°C.

A comparison of the vertical line integral of water vapor (or precipitable water) as derived from the rawinsonde and radiometer is given in Fig. 6. The general agreement in the two measurements is apparent, but the rms difference of 0.32 cm is significantly larger than the predicted value of about 0.1 cm. Similar results have been reported by Staelin *et al.* (1976) and Grody (1976) for the measurement of water vapor from satellites, where rms differences between radiometer and rawinsonde are about 0.4 cm compared with predicted values of about 0.2 cm. These

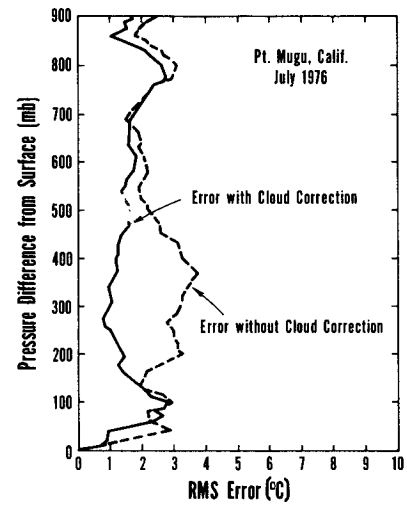

FIG. 4. Experimentally observed accuracies of temperature profiles using a five-channel radiometer with and without correction for radiation from clouds.

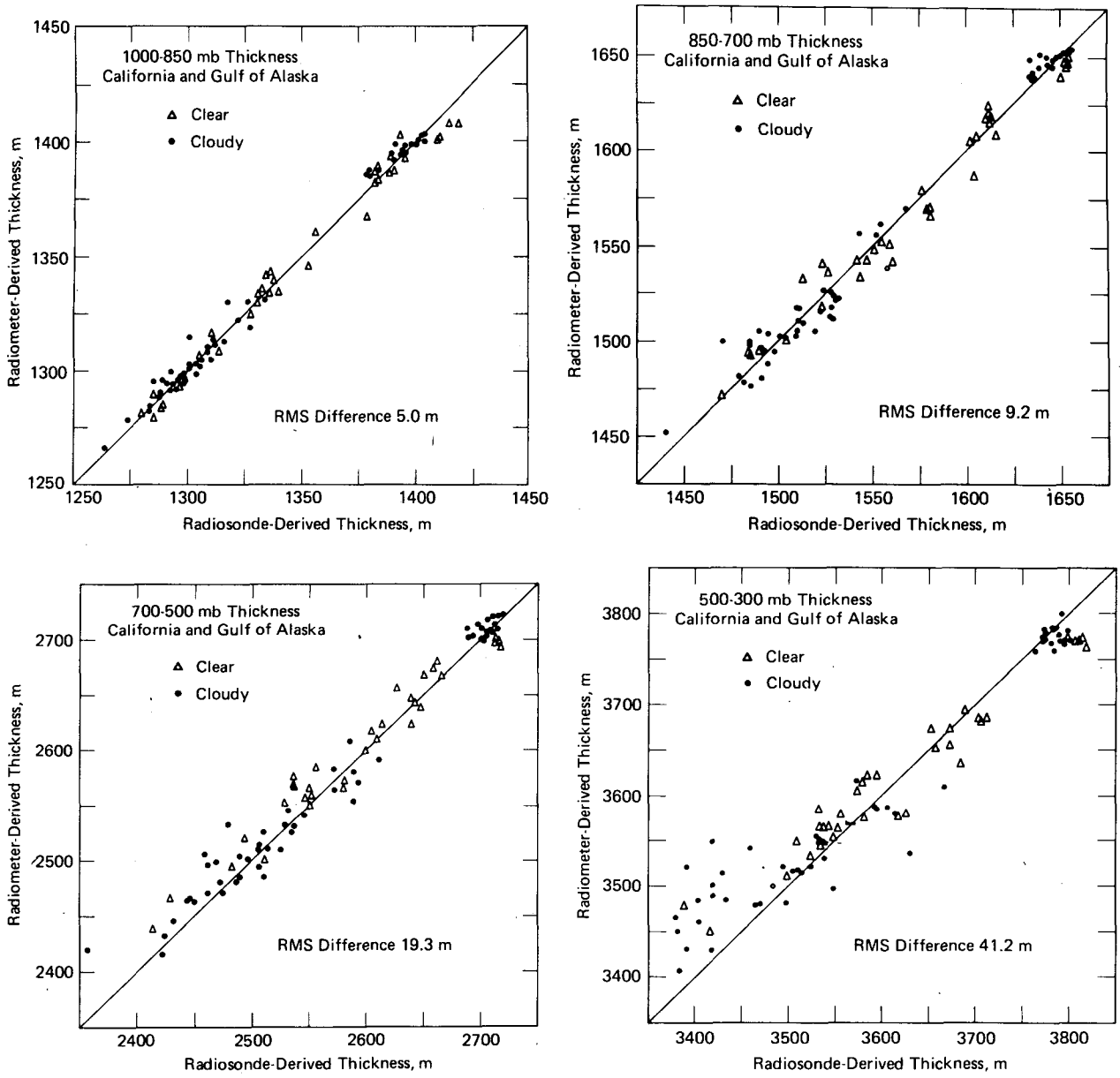

FIG. 5. Comparison of layer thicknesses as derived from rawinsonde and radiometer.

discrepancies could arise from a number of sources, including inaccuracies in the radiometric and rawinsonde measurements and, in the satellite case, errors in earth surface emissivity and temperature. Uncertainties in the absorption coefficient of water vapor may also be a significant source of error.

6. Conclusion

Temperature profiles retrieved from ground-based microwave radiometric measurements under both clear and cloudy conditions have been compared with rawinsonde profiles to show that reasonable agreement with predicted accuracy has been achieved. Root-mean-square accuracies between 1 and 2°C for the mean temperature between standard pressure levels up to 500 mb were obtained for the combined data from the three experimental periods. Measurements with these accuracies will be useful in numerical weather prediction, especially in data-sparse regions.

Water vapor profiles and line integrals from the radiometric data have also been compared with rawinsonde data, but differences of these quantities are somewhat larger than expected. It is likely that discrepancies arise partly from inaccuracies in the rawinsonde itself and partly from uncertainties in our knowledge of water vapor absorption coefficients.

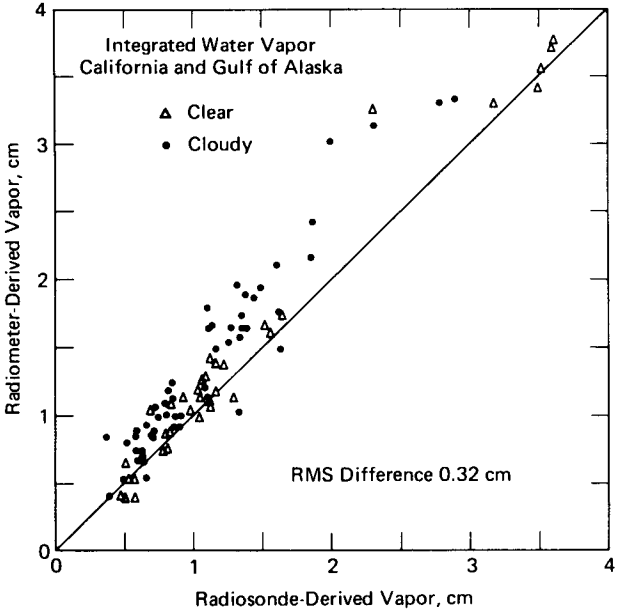

FIG. 6. Comparison of the line integral of water vapor as derived from rawinsonde and radiometer.

Acknowledgments. The radiometric measurements reported here were made under the direction of B. L. Gary and N. I. Yamane of the Jet Propulsion Laboratory, Pasadena, California, with support from the NOAA Data Buoy Office. We express our appreciation to personnel of the Geophysics Division of the Pacific Missile Test Center and of the Canadian Ship *Quadra* for providing meteorological data and facilities for the experiments.

REFERENCES

Fowler, M. G., N. D. Sze and N. E. Gaut, 1975: The estimation of clear sky emission values from cloudy radiometric data. Air Force Cambridge Research Laboratories, TR-75-0440, 57 pp.

Grody, Norman C., 1976: Remote sensing of atmospheric water content from satellites using microwave radiometry. *IEEE Trans. Antennas Propag.*, **AP-24**, 155–162.

Gurvich, A. C., and A. T. Yershov, 1976: On remote determination of anomalous distributions of atmospheric temperature and moisture. *Izv. Acad. Nauk USSR Atmos. Ocean. Phys.*, **12**, 1320–1323.

Hosler, C. R., and T. J. Lemmons, 1972: Radiometric measurements of temperature profiles in the planetary boundary layer. *J. Appl. Meteor.*, **11**, 341–348.

Miner, G. F., D. D. Thornton and W. J. Welch, 1972: The inference of atmospheric temperature profiles from ground-based measurements of microwave emission from atmospheric oxygen. *J. Geophys. Res.*, **77**, 975–991.

Rodgers, C. D., 1970: Remote sounding of the atmospheric temperature profile in the presence of cloud. *Quart. J. Roy. Meteor. Soc.*, **96**, 654–666.

Smith, W. L., H. M. Woolf and W. J. Jacob, 1970: A regression method for obtaining real-time temperature and geopotential height profiles from satellite spectrometer measurements and its application to Nimbus 3 SIRS observations. *Mon. Wea. Rev.*, **98**, 582–603.

Snider, J. B., 1972: Ground-based sensing of temperature profiles from angular and multi-spectral microwave emission measurements. *J. Appl. Meteor.*, **11**, 958–967.

Staelin, D. H., A. H. Barrett, P. W. Rosenkranz, F. T. Barath, E. J. Johnson, J. W. Waters, A. Wouters and W. B. Lenoir, 1975: The scanning microwave spectrometer (SCAMS) experiment. *Nimbus 6 Users Guide*, Goddard Space Flight Center, Greenbelt, Md.

——, K. F. Kunzi, R. L. Pettyjohn, R. K. L. Poon and R. W. Wilcox, 1976: Remote sensing of atmospheric water vapor and liquid water with the Nimbus 5 microwave spectrometer. *J. Appl. Meteor.*, **15**, 1204–1214.

Waters, J. W., K. F. Kunzi, R. L. Pettyjohn, R. K. L. Poon and D. H. Staelin, 1975: Remote sensing of atmospheric temperature profiles with the Nimbus 5 microwave spectrometer. *J. Atmos. Sci.*, **32**, 1953–1959.

Westwater, E. R., J. B. Snider and A. V. Carlson, 1975: Experimental determination of temperature profiles by ground-based microwave radiometry. *J. Appl. Meteor.*, **14**, 524–539.

——, M. T. Decker and F. O. Guiraud, 1976: Feasibility of atmospheric temperature sensing from ocean data buoys by microwave radiometry. NOAA Tech. Rep. ERL 375-WPL 48 [NTIS No. 262–421].

Yershov, A. T., Yu. V. Lebskiy, A. P. Naumov and V. M. Plechkov, 1975: Determination of the vertical temperature profile from ground-based measurements of the atmospheric radiation at $\lambda = 5$ mm. *Izv. Acad. Nauk USSR Atmos. Ocean. Phys.*, **11**, 1220–1229.